SUPPLEMENTAL MATERIAL

Supplemental Methods

Study cohort and myocardial sample collection

HCM patients. 27 HCM patients underwent septal myectomy for clinical indications at Stanford Medical Center. Inclusion criteria: normal or hyperdynamic LV function (left ventricular ejection fraction (LVEF) ≥ 55%) with either eccentric or concentric LV hypertrophy on echo and a gradient across the left ventricular outflow tract (LVOT). Patients were excluded if they had prior evidence of myocardial infarction, primary valvular disease or had progressed to LV dysfunction. A family history of cardiac related disease was obtained and defined as the presence of one or more affected family members with either HCM, arrhythmia, sudden cardiac death, or heart failure. The Stanford Institutional Review Board approved the study.

Controls. Myocardial tissue from both interventricular septum and left ventricular apex were obtained from 13 donor hearts with no major cardiac history, maximum travel distance to Stanford <60 miles, donor ischemic time <6 hours and no history of blunt chest trauma. Because of the difficulty in obtaining fresh control tissue for mitochondrial respiration studies, myocardial tissue from the left ventricular free wall of an additional 2 patients with primary mitral stenosis and not greater than mild mitral insufficiency who were undergoing mitral valve repair or replacement were also used as controls, however these were used for oxygraph respiration studies only.

Cardiac tissue was excised, and a mid-myocardial portion was used immediately for studies of mitochondrial respiration or fixed in 4% paraformaldehyde (PFA) for paraffin

embedding or in 4% PFA and 2% glutaraldehyde for TEM analysis. The remaining tissue was flash frozen in liquid nitrogen for all other assays.

Echocardiography

Echocardiogram reports were reviewed on all patients. Standard measurements of cardiac anatomy and function were performed with M-mode, 2D and pulsed-wave Doppler according to established guidelines[89]. LVEF was calculated by the biplane Simpson method in the apical four- and two-chamber views. Parasternal short axis views were used to measure maximum wall thickness. Left ventricular outflow tract (LVOT) obstruction, defined as a gradient of >30 mmHg measured at rest, was recorded by Doppler. Exercise LVOT gradients were also recorded in 25 patients. LV mass and LV mass index was calculated by ASE method[90] in 24 patients.

MRI and fibrosis quantification

Left ventricular mass (LV mass) was calculated from MRI and indexed to body surface area in 9 patients. Percent fibrosis was determined by myocardial delayed enhancement (MDE) in 9 HCM patients, using three different methods: qualitatively (0=no delayed enhancement, 1=mild delayed enhancement signal, 2=prominent delayed enhancement signal), quantitatively using QMass version 8.1 (Medis, Leiden, Netherlands) as well as by area of signal higher than 5 standard deviations of signal in an area without delayed enhancement, processed twice using different regions.

Genetic evaluation and DNA sequencing

Twenty-five patients received genetic counselling after analysis of arrythmia and cardiomyopathy-associated gene-panels from the Stanford Center for Inherited Cardiovascular Disease. Variants were classified in 3 different classes: pathogenic, likely pathogenic, and variant of unknown significance (VUS) based on ClinVar, GeneDx, and Invitae scoring **(Table III** in the Supplement**)**. We performed DNA-Sequencing on four patients who were missing genetic information using the Ion Torrent platform (Thermo Fisher, Waltham, MA). Briefly, genomic DNA was isolated using DNeasy (Qiagen, Valencia, CA). Ion Torrent libraries were prepared with the Ion AmpliSeqKit for Chef DL8 (Thermo Fisher Scientific) using a custom AmpliSeq panel (Thermo Fisher Scientific), that covers 135 cardiomyopathy and congenital heart disease DNA panel genes associated with sudden cardiac death. Next, the libraries were sequenced on an Ion PIChip (Thermo Fisher Scientific) with the Ion Proton system using the Ion PI™ Hi-QSequencing 200 Kit (Thermo Fisher Scientific). Sequence reads were aligned to human genome hg19 using Ion Torrent Suite Software (v5.0) and genomic variants were detected by Torrent Variant Caller plugin. Variant call format (VCF) file of each sample was annotated by Ion Reporter (ionreporter.thermofisher.com). Functional annotations of genetic variants were performed by ANNOVAR software as previously described[91].

Histological assessments

Fresh myocardial tissue samples (HCM, n=7; control, n=7) were washed with normal saline solution followed by fixation in 4% paraformaldehyde (PFA) for 24h. The tissue was then embedded in paraffin and sectioned to 7µm thickness. After deparaffinization, adjacent sections were stained with hematoxylin and eosin (H&E) to assess tissue

morphology and Masson trichrome for collagen deposition associated with fibrosis. All images were taken with a Keyence microscope (BZ-9000, Keyence, Osaka, Japan). Fibrotic area was quantified by comparing the area of tissue stained blue (collagen) to the total tissue area using MIPAR software as previously described[92].

Metabolomic and Lipidomic analysis

Sample Preparation. Roughly 30 mg of frozen heart tissue were homogenized in 500 µl ice-cold methanol by bead beating (MP bioscience cat# 6913-100, Solon, OH) at 4°C (2 x 45 s). Metabolites and complex lipids were extracted using a biphasic separation with cold methyl tert-butyl ether (MTBE), methanol and water. Briefly, 1 ml of ice-cold MTBE was added to 300 µl of the homogenate spiked-in with 40 µl deuterated lipid internal standards (Sciex, cat#: 5040156, lot#: LPISTDKIT-101). The samples were then sonicated (3 x 30 s) and agitated at 4°C for 30 min. After addition of 250 µl of ice-cold water, the samples were vortexed for 1 min and centrifuged at 14,000 g for 5 min at 20°C. The upper organic phase contains the lipids, the lower aqueous phase contains the metabolites and the proteins are precipitated at the bottom of the tube. For quality controls, 3 reference plasma samples (40 µl plasma) and 1 preparation blank were processed in parallel.

1) *Metabolites:* Proteins were further precipitated by adding 700 µl of 33/33/33 acetone/acetonitrile/methanol spiked-in with 15 labeled metabolite internal standards to 300 µl of the aqueous phase and 200 µl of the lipid phase and incubating the samples

overnight at -20°C. After centrifugation at 17,000 g for 10 min at 4°C, the metabolic extracts were dried down to completion and resuspended in 100 µl 50/50 methanol/water.

2) Complex lipids: 700 µl of the organic phase was dried down under a stream of nitrogen and resolubilized in 200 µl of methanol for storage at -20°C until analysis. The day of the analysis, samples were dried down, resuspended in 300 µl of 10 mM ammonium acetate in 90/10 methanol/toluene and centrifuged at 16,000 g for 5 min at 24°C.

Data acquisition. Metabolite extracts were analyzed using a broad-spectrum untargeted LC-MS platform as previously described[93] while complex lipids were quantified using a targeted MS-based approach[94]. Cardiolipins were not measured as part of the targeted method, so the lipid extracts were further analyzed using an untargeted LC-MS approach[94].

1) Untargeted Metabolomics by Liquid Chromatography (LC)-MS. Metabolic extracts were analyzed four times using HILIC and RPLC separation in both positive and negative ionization modes. Data were acquired on a Thermo Q Exactive HF mass spectrometer for HILIC (Thermo Fisher Scientific, Bremen, Germany) and a Thermo Q Exactive mass spectrometer for RPLC (Thermo Fisher Scientific, Bremen, Germany). Both instruments were equipped with a HESI-II probe and operated in full MS scan mode. MS/MS data were acquired on quality control samples (QC) consisting of an equimolar mixture of all samples in the study. HILIC experiments were performed using a ZIC-HILIC column 2.1 x 100 mm, 3.5 µm, 200Å (Merck Millipore, Darmstadt, Germany) and mobile phase

solvents consisting of 10 mM ammonium acetate in 50/50 acetonitrile/water (A) and 10 mM ammonium acetate in 95/5 acetonitrile/water (B). RPLC experiments were performed using a Zorbax SBaq column 2.1 x 50 mm, 1.7 µm, 100Å (Agilent Technologies, Palo Alto, CA) and mobile phase solvents consisting of 0.06% acetic acid in water (A) and 0.06% acetic acid in methanol (B). Data quality was ensured by (i) injecting 6 and 12 pool samples to equilibrate the LC-MS system prior to running the sequence for RPLC and HILIC, respectively, (ii) injecting a pool sample every 10 injections to control for signal deviation with time, and (iii) checking mass accuracy, retention time and peak shape of internal standards in each sample.

2) Targeted Lipidomics using the Lipidyzer Platform. Lipid extracts were analyzed using the Lipidyzer platform[94] that comprises a 5500 QTRAP system equipped with a SelexION differential mobility spectrometry (DMS) interface (Sciex) and a high flow LC-30AD solvent delivery unit (Shimazdu, Columbia, MD). Briefly, lipid molecular species were identified and quantified using multiple reaction monitoring (MRM) and positive/negative ionization switching. Two acquisition methods were employed covering 10 lipid classes; method 1 had SelexION voltages turned on while method 2 had SelexION voltages turned off. Data quality was ensured by i) tuning the DMS compensation voltages using a set of lipid standards (cat# 945 5040141, Sciex) after each cleaning, more than 24 hours of idling or 3 days of consecutive use, ii) performing a quick system suitability test (QSST) (cat# 50407, Sciex) before each batch to ensure acceptable limit of detection for each lipid class, and iii) triplicate injection of lipids extracted from a reference plasma sample (cat# 948 4386703, Sciex) at the beginning of the batch.

3) Untargeted Lipidomics by LC-MS. Lipid extracts were also analyzed using an Ultimate 3000 RSLC system coupled with a Q Exactive mass spectrometer (Thermo Scientific, Waltham, MA) as previously described[94]. Each sample was run twice in positive and negative ionization modes. Lipids were separated using an Accucore C18 column 2.1 x 150 mm, 2.6 µm (Thermo Scientific) and mobile phase solvents consisted in 10 mM ammonium acetate and 0.1% formic acid in 60/40 acetonitrile/water (A) and 10 mM ammonium acetate and 0.1% formic acid in 90/10 isopropanol/acetonitrile (B). The Q Exactive was equipped with a HESI-II probe and operated in data-dependent acquisition mode for all the samples. To maximize the number of identified lipids, the 100 most abundant peaks found in blanks were excluded from MS/MS events. Data quality was ensured by (i) injecting 6 pool samples to equilibrate the LC-MS system prior to running the sequence, (ii) injecting a pool sample every 10 injections to control for signal deviation with time, and (iii) checking mass accuracy, retention time and peak shape of internal standards in each sample.

Data processing.

Metabolomics. Data from each mode were independently analyzed using Progenesis QI software (v2.3) (Nonlinear Dynamics, Durham, NC). Metabolic features from blanks and those that didn't show sufficient linearity upon dilution in QC samples ($r<0.6$) were discarded. Only metabolic features present in >2/3 of the samples were kept for further analysis. Median normalization was applied to correct for differential starting material quantity. Missing values were imputed by drawing from a random distribution of low values in the corresponding sample. Data from each mode were merged and metabolites

of interest were formally identified by matching fragmentation spectra and retention time to analytical-grade standards when possible or matching experimental MS/MS to fragmentation spectra in publicly available databases. In total, 267 metabolites were formally identified. We used the Metabolomics Standards Initiative (MSI) level of confidence to grade metabolite annotation confidence (level 1 - level 4) **(Excel II** in the Supplement**)**. Level 1 represents formal identifications where the biological signal matches accurate mass, retention time and fragmentation spectra of an authentic standard run on the same platform. For level 2 identification, the biological signal matches accurate mass and fragmentation spectra available in METLIN database. Acylcarnitines, free fatty acids and complex lipids don't necessarily all have MS/MS data in public databases but were annotated based on expected signature fragments. Level 3 represents putative identifications that are the most likely name based on previous knowledge. Level 4 consists in unknown metabolites. Metabolite abundances were reported as spectral counts.

Targeted Lipidomics. Lipidyzer data were reported by the Lipidomics Workflow Manager (LWM) software which calculates concentrations for each detected lipid as average intensity of the analyte MRM/average intensity of the most structurally similar internal standard (IS) MRM multiplied by its concentration. Lipid abundances were reported as concentrations in nmol/g. Lipids detected in less than 2/3 of the samples were discarded and missing values were imputed by drawing from a random distribution of low values class-wise in the corresponding sample. Median normalization (excluding TAG and DAG) was applied to correct for differential starting material quantity. Lipid abundances were reported as concentrations in nmol/g.

Untargeted Lipidomics. LC-MS peak extraction, alignment, quantification and annotation was performed using LipidSearch software version 4.2 (Thermo Scientific). Only lipids present in >2/3 of the samples were kept for further analysis. Median normalization (excluding TAG and DAG) was applied to correct for differential starting material quantity. Missing values were imputed by drawing from a random distribution of low values in the corresponding sample. Lipids were identified by matching the precursor ion mass to a database and the experimental MS/MS spectra to a spectral library containing theoretical fragmentation spectra. The identity of cardiolipins, detected as [M-H]-, was manually validated by investigating individual MS/MS spectra. Lipid abundances were reported as spectral counts.

Data analysis.

Differential analysis was performed using a non-parametric Welsh t-test (two sided) on log2-transformed data. P values were corrected for multiple hypothesis using the Benjamini-Hochberg method and analytes with FDR below 0.05 were considered significant. Since our current method to measure phosphonucleotide (ATP, PCr, ADP) was not quantitative and these molecules could probably ionize differently, we did not compare their signals (e.g., ATP:ADP ratio) in our study. Metabolomics and untargeted lipidomics data were deposited to Metabolomics Workbench and were assigned the following accession numbers: ST001886 and ST001887 respectively.

RNA sequencing

Sample Preparation. RNA was isolated from the frozen tissue using RNeasy Plus Micro kit (Qiagen, Valencia, CA). Quality and integrity of total RNA was measured on Agilent Technologies 2100 Bioanalyzer (Agilent Technologies). RNA sequencing library was constructed using NEBNext® Ultra II RNA Library Prep Kit (New England Biolabs, Beverly, MA) according to manufacturer's protocols. Briefly, mRNA was purified from total RNA using poly-T oligo-attached magnetic beads. The mRNA is first fragmented randomly by addition of fragmentation buffer. Then first strand cDNA is synthesized using random hexamer primer and M-MuLV Reverse Transcriptase (RNase H-). Second strand cDNA synthesis is subsequently performed using DNA Polymerase I and RNase H. Double-stranded cDNA is purified using AMPure XP beads. Remaining overhangs of the purified double-stranded cDNA are converted into blunt ends via exonuclease/polymerase activities. After adenylation of 3' ends of DNA fragments, NEBNext Adaptor with hairpin loop structure is ligated to prepare for hybridization. In order to select cDNA fragments of preferentially 150~200 bp in length, the library fragments are purified with AMPure XP system (Beckman Coulter, Brea, CA). Finally, the final library is produced by PCR amplification and purification of PCR products by AMPure XP beads. Library concentration was quantified using a Qubit 2.0 fluorometer (Life Technologies), and then diluted to 1ng/μl before checking insert size on an Agilent Technologies 2100 Bioanalyzer (Agilent Technologies). The library was then quantified to greater accuracy by quantitative PCR (qPCR). Each library was sequenced by in paired end mode with read length 2 × 150 bp. On average, we generated 36 million

paired-end reads for each sample in a fraction of a sequencing lane on Illumina NovaSeq 6000 system.

Data acquisition/analysis. Downstream analysis was performed using a combination of programs including STAR, HTseq, Cufflink and our wrapped scripts. Alignments were parsed using Tophat and differential expressions were determined through DESeq2/edgeR (Wald test with FDR corrected $p<0.05$). Gene Ontology (GO), Kyoto and Enrichment analysis (DO), and Reactome enrichment were implemented by the ClusterProfiler. GOPlot[95] was used to better visualize relationships between genes and enriched canonical pathways. Selected heatmaps were generated using open-source Morpheus platform (https://software.broadinstitute.org/morpheus/). Pearson correlation coefficient heatmaps were plotted using cluster map' function in Python's Seaborn library. The RNA-Seq data was uploaded to GEO and were assigned accession number: GSE180313.

Integrated analysis using metabolites, lipids, and transcripts

Pathway enrichment analysis. We used the open source web tool IMPaLA[96] to search for enriched pathways using differentially expressed metabolites, lipids, and transcripts (FDR<0.05). All the detected metabolites, and transcripts were used as background. Significance of pathways was determined by the Fisher's method. P values were corrected for multiple hypothesis using the Benjamini-Hochberg method and pathways with FDR below 0.05 were considered significant.

Network analysis. A basic network of metabolites, lipids, and transcripts was built through the GAM web-service (https://artyomovlab.wustl.edu/shiny/gam/)[97] and Cytoscape 3.4.0 (http://www.cytoscape.org/) to visualize the connection among the metabolites and associated enzymes. Key software/web-based platforms used here are listed in **Table I** in the Supplement.

Transmission electron microscopy (TEM)

Fresh myocardial tissue samples were cut into pieces of ~1 mm3 and washed with PBS. Three pieces of tissue from each sample were further processed for EM analysis. Samples were then fixed in Karnovsky's fixative: 2% Glutaraldehyde (EMS Cat# 16000) and 4% Formaldehyde (EMS Cat# 15700) in 0.1M Sodium Cacodylate (EMS Cat# 12300) pH 7.4 for 1 hr then moved to 4oC. The fix was replaced with cold/aqueous 1% Osmium tetroxide (EMS Cat# 19100) and then allowed to warm to Room Temperature (RT) for 2 hrs rotating in a hood, washed 3X with ultra-filtered water, then the block stained in 1% Uranyl Acetate at RT 2hrs while rotating. Samples were then dehydrated in a series of ethanol washes for 30 minutes each at RT beginning at 50%, 70% EtOH then moved to 4oC overnight. They were place in cold 95% EtOH and allowed to warm to RT, changed to 100% 2X, then Propylene Oxide (PO) for 15 min. Samples are infiltrated with EMbed-812 resin (EMS Cat#14120) mixed 1:2, 1:1, and 2:1 with PO for 2 hrs. each with leaving samples in 2:1 resin to PO overnight rotating at RT in the hood. The samples are then placed into EMbed-812 for 2 to 4 hours then placed into molds w/labels and fresh resin, orientated and placed into 65o C oven overnight. Thin sections (80 nm) were cut using a Leica EM UC7 Ultramicrotome (Leica Microsystems) and placed on 100 mesh copper

grids (Electron Microscopy Sciences). Sample grids were post-stained in 1.5% Uranyl Acetate in 50% Acetone for 30 seconds, washed and dried then stained 2 minutes in Sato's lead citrate, observed with a JEM-1400 transmission electron microscope (JEOL) operating at 120 kV. From each tissue section 40-50 fields were randomly picked and captured on Gatan Orius 832 digital camera (Gatan, Pleasanton, CA).

Individual intermyofibrillar (IMF) mitochondria were then manually traced using ImageJ (NIH) software at a magnification of X3000. The following mitochondrial morphology and shape descriptors were then quantified in each image (n=15-20 images/group) and averaged for each sample: area (in μm2), perimeter (μm), content (total mitochondria area/image area*100), circularity (4π (surface area/perimeter2)), Feret's diameter (longest distance (μm) between any two points within a given mitochondrion, aspect ratio (major axis/minor axis; a measure of the "length to width ratio") and form factor (perimeter/4π·surface area; a measure sensitive to the complexity and branching aspect of mitochondria)[98]. Additionally, we manually assessed cristae density of individual mitochondria within each image. Mitochondria full of normal appearing cristae (~100%) were scored as healthy while mitochondria which had lost less than 50% cristae density were scored as moderately damaged and those that had lost more than 50% cristae density were scored as severely damaged. All quantifications were done blinded to sample identification.

SerialEM imaging

Serial sections were taken around 80nm, picked up on formvar/Carbon coated slot Cu grids, stained for 40seconds in 3.5% Uranyl Acetate in 50% Acetone followed by staining in 0.2% Lead Citrate for 4 minutes. Observed in the JEOL JEM-1400 120kV, EM-21010 holder with the high tilt removeable tip: EM-21311HTR. Tilt series were taken using a Gatan Orius 832 4k X 2.6k digital camera with 9um pixel size in conjunction with SerialEM software (bio3d.colorado.edu) collecting image stacks at 1.5-degree tilts between -65 degrees to +65 degrees.

Tomogram reconstruction and annotation

Tilt series from serial sections were individually aligned and reconstructed into tomograms using the weighted back-projection algorithm in the IMOD software package[99,100]. The serial tomograms were then aligned and joined to obtain the final volume in IMOD. The cristae and the mitochondrial membrane in the joined volume were annotated semi-automatically using the convolutional neural network algorithm in EMAN2[101]. All surface visualizations were done in UCSF ChimeraX[102].

mtDNA/NucDNA quantification

DNA was isolated from LV samples using Qiagen DNA extraction kit (Cat# 69504). Mitochondrial DNA content was analyzed by quantitative real-time polymerized chain reaction with Human mitochondrial DNA (mtDNA) monitoring primer pet (Cat# 7246, Takara). The ratio of the mitochondrial-encoded NADH dehydrogenase-1 and 5 (*ND1* and

ND5) to the nuclear-encoded *SLCO2B1* and *SERPINA1* genes were assessed using the ΔΔCT method and the relative fold change was normalized to normal donors.

Protein isolation, western blotting, and enzyme-linked immunosorbent assay (ELISA)

Fresh frozen ventricular tissue (20 mg) was homogenized in RIPA buffer (Cell Signaling technology, Danvers, MA). Immediately before lysis, a protease and phosphatase inhibitor cocktail (Sigma) were added to the lysis buffer. Samples were centrifuged at 1000g for 15 minutes at 4°C, and supernatant was collected for further analysis. Protein concentrations were determined using the BCA Protein Assay Kit (ThermoScientific). For western blotting, equal amount of protein (~30 µg) was separated by 10% sodium dodecyl sulphate-polyacrylamide gel electrophoresis (SDS-PAGE) and transferred onto a 0.45 um nitrocellulose membrane. Equal loading in each lane was confirmed by staining the blots with Ponceau S (2%). Nitrocellulose membranes were then immersed in PBS containing 5% skimmed milk and 0.1% Tween 20 (blocking solution) for 1 h at room temperature, cut into strips and incubated with monoclonal antibodies associated with mitochondrial dynamics, mitophagy, ROS and AMP kinase activation (summarized in **Table II** in the Supplement**)** overnight at 4°C. Thereafter, the strips were incubated for with horseradish peroxidase-conjugated secondary antibodies (Jackson ImmunoResearch Laboratories, West Grove, PA) for 1h at room temperature. Immunoblots were then visualized with the enhanced chemiluminescence western blot detection kit (Bio-Rad Laboratories, Hercules, CA) and geldoc imager (Bio-Rad) and quantified with ImageJ software. ELISA was used to measure p-AMPK (Abcam, cat# 7959C) in accordance with the instructions

of each kit. Briefly, hearts were thoroughly rinsed in PBS to remove blood, followed by mechanical homogenization with an extraction buffer in a 1:5 ratio (tissue:extraction buffer), incubated for 20 min on ice, and then centrifuged at 11,000 × g at 4 °C for 10 min. Subsequently, the supernatants were diluted in an incubation buffer in a 1:4 ratio (supernatant:incubation buffer) and used for ELISA reactions. Absorbance was measured at 550 nm with a microplate reader (Synergy HT, BioTek Instruments, Winooski, VT).

Isolation of mitochondria

Tissue was minced and thoroughly rinsed with ice-cold PBS. The tissue was gently homogenized using a Dounce homogenizer (20 strokes) in isolation buffer (300mM sucrose, 10mM hepes, 2mM EGTA, pH 7.2, 4°C). Tissue lysates were then placed on ice for differential centrifugation. Tissues were centrifuged at 500 x g for 10 min and the resulting supernatants were centrifuged at 10,000 x g for 15 min. The mitochondrial pellet was washed once with isolation buffer and the final pellet resuspended in a minimal volume of isolation buffer. For western blot analysis, mitochondria were solubilized in isolation buffer containing 1% Triton X and stored at -80°C. Mitochondrial protein concentration was measured using a BCA assay (Pierce, Rockford, IL) in duplicate. Purity of mitochondrial fractions was confirmed by the absence of the cytosolic protein enolase.

Mitochondrial respiratory measurement

Myocardial tissue samples (5 mg) were gently minced using a scissor in ice-cold oxygraph buffer (20 mM HEPES, 5 mM K3PO4, 0.2 mM EDTA, 2.5 mM MgCl2, 10 mM KCl, 0.25 M sucrose, 1 mg/mL fatty acid free-bovine serum albumin; pH 7.4). High resolution

respirometry (Oroboros Oxygraph 2K, Oroboros Instruments, Innsbruck, Austria) was used to measure respiration in response to different substrates as previously described[103]. Briefly, complex I-NADH dehydrogenase activity was measured in response to malate (2.5 mM) and glutamate (5 mM). Oligomycin (2.5 µg/mL), complex V inhibitor, was used to assess leak respiration. Oxidative phosphorylation was assessed in response to the substrate ADP (1.5 mM) to evaluate Complex V (ATP synthase) activity. Uncoupled respiration was assessed in response to FCCP (Carbonyl cyanide-p-trifluoromethoxyphenylhydrazone, 0.5 µM) to evaluate the maximal electron transport chain (ETC) activity. Antimycin A (2.5 µM) was used to abolish the ETC activity. We further analyzed the respiratory control ratios (RCR) to evaluate the OXPHOS efficiency. The oxygen consumption rates are reported as O2 flux per volume (pmol/s/mL) by Datlab2 software (Oroboros Instruments, Innsbruck, Austria). The reagents are listed in **Table II** in the Supplement.

Mitochondrial enzymatic and complexes activity assays

Mitochondrial respiratory chain enzyme and citrate synthase (CS) activities were determined by spectrophotometric enzyme assay. Briefly, complex I activity was immediately measured on a DU800 spectrophotometer using 2,6-dichloroindophenol (DCIP) as the terminal electron acceptor at 600 nm with the oxidation of NADH reducing artificial substrates Coenzyme Q10 that then reduces DCIP[104]. The reduction of DCIP is mostly dependent on complex I activity and has a very high rotenone sensitive activity. Complex II activity was analyzed as the reduction of dichloroindophenol at 600 nm with succinate as the substrate. Complex IV activity was measured by the oxidation of

cytochrome c at 550 nm[105]. Data are represented as the pseudo first order rate constant (k) divided by protein concentration. ATP synthase activity, measured in the direction of ATP hydrolysis (ATPase activity), was assayed by the continuous spectrophotometric monitoring of the oxidation of NADH (e340 = 6180 M-1cm-1) in an enzyme-linked ATP regenerating assay using ATP, phosphoenolpyruvate, pyruvate kinase, and lactate dehydrogenase to determine the ATPase activity (NADH loss) in nmol/min/mg protein[106,107]. Citrate synthase was measured using the coupled reaction with oxaloacetate, acetyl-CoA, and 5,5-dithiobis-(2,4-nitrobenzoic acid)[108].

Glutathione peroxidase (GPx) activity assay

GPx activity was measured using Cayman glutathione peroxidase assay kit (Cayman Chemicals, Ann Arbor, MI) according to the manufacturer's instructions. Briefly, homogenized tissue was centrifuged at 10,000 x g for 15 min at 4 °C to obtain the cytoplasmic fraction. Equal amount of protein fractions was incubated with reaction mixture containing the tetrazolium salt for 20 min. The absorbance of each standard and sample was read at 450 nm using a 96-well Microplate Reader. GPx activity was calculated using the linear regression fit of the standard curve data. All assays were run in duplicate.

Supplemental Table I

List of key software/web-based platforms.

	Source	Identifier
Software/web-based platforms		
FIJI	NIH	https://fiji.sc/
GraphPad Prism	GraphPad Software 8.0	https://www.graphpad.com/scientific-software/prism/
Morpheus	Broad Institute	https://software.broadinstitute.org/morpheus/
GAM Shiny	Artyomov lab at Washington University	https://artyomovlab.wustl.edu/shiny/gam/
Cytoscape	Institute of Systems Biology in Seattle	https://cytoscape.org/
IMPaLA	Max Planck Institute for Molecular Genetics	http://impala.molgen.mpg.de/
MIPAR	image analysis software	https://www.mipar.us/applications-histology.html

Supplemental Table II

List of reagents and chemicals.

Reagents or resources	Source	Identifier
Antibodies		
Mouse Anti human AMPK	CST	2532
Phospho-AMPKα (Thr172)	CST	2535
DRP1	CST	8570
p637DRP1	CST	4867
p616DRP1	CST	4494
MFN2	CST	9482
Endolase	CST	3810
Anti-VDAC1 / Porin	CST	ab14734
LC3	CST	4108
4-HNE	US Bio	H6275-02
OPA1	Abcam	ab42364
CPT1	Abcam	ab128568
SQSTM1/p62	CST	5114S
Parkin	SC	sc-32282
PGC1	Abcam	ab188102
PKM	Abcam	ab38237
GAPDH	Advanced ImmunoChemical	2-RGM2
Chemicals		
RIPA Buffer	Sigma	R0278
Malate	Sigma	240176
Glutamate	Sigma	G1626
ADP	Sigma	A4386
FCCP	Sigma	C2920
Oligomycin	Sigma	O4876
AntimycinA	Sigma	A8674
Hepes	Sigma	H7523
BSA	Sigma	A6003
MgCl2	Sigma	M9272
KH2PO4	Merck	104873
KCl	Merck	104936
Critical Commercial Assays		
DNeasy Blood & Tissue Kit	Qiagen	69504
RNeasy Plus Micro Kit	Qiagen	74034
CST PathScan Phospho-AMPKα (Thr172) Sandwich ELISA Kit	CST	7959C
Human Mitochondrial DNA (mtDNA) Monitoring Primer Set	Takara	7246
Glutathione Peroxidase Assay Kit	Cayman Chemical	703102
iTaq™ Universal SYBR ® Green Supermix	Bio-Rad	1725124

Supplemental Table III

Detailed characteristics of HCM subjects.

	Demographics			Medication			Echocardiogram					Mutation info
ID	Sex	Age (year)	Positive Family Hx (y/n)	β-blocker	Calcium channel blocker	Statin	LVEF (%)	IVSd (cm)	LVPWd (cm)	IVSd : LVPWd ratio	LVOT rest grad, (exercise or Valsalva grad) (mmHg)	Classification (ClinVar/GeneDx/Invitae)
				(y/n)								
H1	M	65	n	n	y	y	55	1.9	1.9	1.0	133 (133)	No mutation detected
H2	M	68	y	y	n	y	58	1.9	1.9	1.0	54 (117)	-
H3	M	24	n	n	n	n	>75	1.7	1.2	1.4	86 (150)	NM_000257.4 **MYH7** p.Ser738Thr (Likely pathogenic)
H4	M	43	n	y	n	n	66	1.8	1.5	1.2	47 (101)	NM_003476.5 **CSRP3** p.Thr179Met (Likely pathogenic)
H5	F	67	n	y	y	n	68	1.5	1.5	1.0	112 (216)	NM_000256.3 **MYBPC3**p.Arg502Trp (Pathogenic)
H6	M	32	n	n	y	n	65	1.7	1.4	1.2	80 (147)	No mutation detected
H7	M	65	y	n	n	n	75	0.8	1.0	0.8	45 (135)	NM_000257.4 **MYH7** p.Arg663His (Pathogenic)
H8	M	50	n	n	y	n	70	2.6	1.4	1.9	33 (-)	NM_000256.3 **MYBPC3** p.Ala364Thr (Pathogenic)
H9	M	50	n	y	y	n	67	1.9	1.6	1.2	21 (120)	No mutation detected
H10	M	53	n	n	y	y	60	1.5	1.5	1.0	12 (106)	NM_000257.4 **MYH7** p.Val1213Met (VUS)
H11	M	46	n	n	y	n	64	2.4	1.1	2.2	29 (146)	NM_000257.4 **MYH7** p.Asn1327Lys (VUS) NM_000256.3 **MYBPC3** p.Glu1179Lys (VUS)
H12	M	60	n	n	y	y	66	1.8	1.4	1.3	20 (73)	No mutation detected
H13	M	48	y	y	y	y	57	2.8	0.9	3.1	65 (100)	NM_000256.3 **MYBPC3** p.Trp792Arg (Likely pathogenic) NM_000364.4 **TNNT2** p.Arg285Cys (Likely pathogenic)
H14	M	72	y	y	n	y	74	2.2	1.5	1.5	46 (99)	No mutation detected
H15	M	54	y	n	y	y	60	2.8	2.2	1.3	12 (106)	No mutation detected
H16	M	55	n	y	n	y	79	2.1	1.9	1.1	15 (100)	No mutation detected
H17	M	36	n	n	y	n	65	1.3	1	1.3	15 (100)	NM_000256.3 **MYBPC3** p.Val219Leu (Pathogenic)
H18*	F	73	n	y	y	y	51	1.1	1.0	1.1	30 (115)	NM_000256.3 **MYBPC3** p.Leu1258Ter (Pathogenic)
H19	M	52	n	n	y	y	65	2.6	1.8	1.4	78 (78)	No mutation detected
H20	M	61	n	n	y	n	65	1.6	1.6	1.0	70 (103)	No mutation detected
H21	M	51	n	n	y	n	70	2.5	1.3	1.9	90 (90)	-
H22	F	72	y	y	n	n	65	1.9	1.1	1.7	77 (96)	No mutation detected
H23	F	66	n	y	y	y	75	1.1	1.1	1.0	24 (54)	No mutation detected
H24	M	23	y	n	n	n	74	1.4	1.2	1.2	57 (106)	NM_000257.4 **MYH7** p.Glu1356Lys (Likely pathogenic)
H25	F	69	n	n	y	y	60	3.1	0.9	3.4	9 (42)	NM_000256.3 **MYBPC3** p.Trp792Arg (Likely pathogenic)
H26	F	63	y	n	y	y	71	1.7	0.9	1.9	50 (120)	NM_000256.3 **MYBPC3** p.Val219Leu (Pathogenic)
H27	M	66	n	y	y	y	71	1.5	0.9	1.5	71 (78)	NM_000335.4 **SCN5A** p.Asp1274Asn (Pathogenic)

*prior unsuccessful alcohol septal ablation.

MYBPC, myosin binding protein C; *MYH7*, myosin heavy chain; *TNNT, troponin T;*

CSRP, cysteine and glycine-rich protein; and *SCN,* sodium voltage-gated channel*;*

VUS, Variant of uncertain significance.

Supplemental Table IV

Characteristics of control subjects.

Group	Research ID	Sex	Age (year)	LVEF (%)	Cause of death
Donor	**D1**	F	62	62	CVA/Stroke
	D2	F	38	65	CVA/Stroke
	D3	F	38	48	CVA/Stroke
	D4	M	56	-	Anoxia
	D5	F	52	61	CVA/Stroke
	D6	F	64	60	CVA/Stroke
	D7	M	48	55	CVA/Stroke
	D8	F	21	60	Anoxia
	D9	M	63	-	Anoxia
	D10	F	57	52	CVA/Stroke
	D11	M	41	-	CVA/Stroke
	D12	F	49	-	CVA/Stroke
	D13	F	42	65	CVA/Stroke
Mitral Stenosis	**MS1**	F	44	65	-
	MS2	F	53	56	-

CVA, cerebrovascular accident

Supplemental Table V

Samples' workflow.

Group	ID	Fibrosis (y/n)		Mass spec (y/n)	RNA-Seq (y/n)	TEM (y/n)	Respiratory measurements (y/n)	Complex activity (y/n)
		Trichrome staining	MRI					
HCM	H1#	n	n	n	n	n	n	n
	H2#	n	n	n	n	n	n	n
	H3	n	y	n	n	n	y	n
	H4	n	n	y	y	n	y	y
	H5	n	y	y	y	y	y	y
	H6	y	n	y	y	y	y	n
	H7	y	n	y	y	y	y	y
	H8	n	n	y	y	n	n	n
	H9#	n	n	n	n	n	n	n
	H10	n	y	n	n	n	n	n
	H11	y	y	y	y	n	n	n
	H12	n	n	n	n	n	n	n
	H13	n	y	y	y	n	n	n
	H14#	n	n	n	n	n	n	n
	H15#	n	n	n	n	n	n	n
	H16	n	n	y	y	y	n	n
	H17	n	n	y	y	y	n	y
	H18	y	n	y	y	y	n	n
	H19	y	n	n	n	n	n	n
	H20	y	n	n	n	y	n	n
	H21	n	n	y	y	y	n	n
	H22	n	n	y	y	y	n	y
	H23	n	y	n	n	y	n	n
	H24	y	y	n	n	y	n	n
	H25	n	y	n	n	y	n	n
	H26	n	y	y	y	y	n	n
	H27	n	n	n	n	y	y	n
Control	D1	y	n	y	n	n	n	n
	D2#	n	n	n	n	n	n	n
	D3	y	n	y	y	n	n	n
	D4#	n	n	n	n	n	n	n
	D5#	n	n	n	n	n	n	n
	D6	n	n	n	y	n	n	n
	D7	y	n	n	n	n	y	n
	D8	y	n	y	y	y	n	n
	D9	y	n	y	y	y	n	y
	D10	y	n	y	y	y	n	y
	D11	y	n	y	y	n	n	y
	D12	n	n	n	y	n	n	y
	D13	n	n	n	n	n	n	y
	MS1	n	n	n	n	n	y	n
	MS2	n	n	n	n	n	y	n

Detailed information of the key assays performed on each sample. #samples were used in other analyses (e.g., western blot).

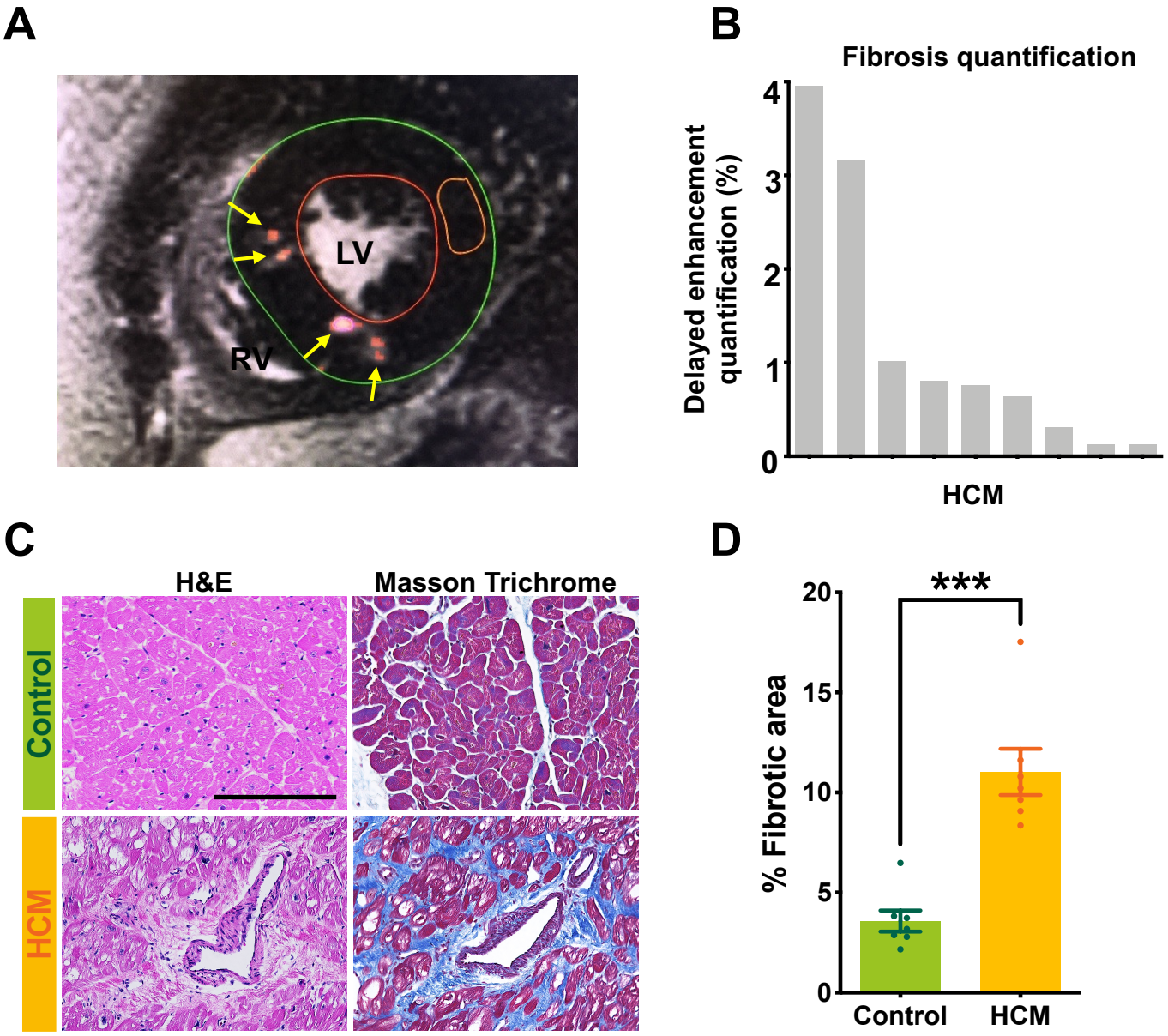

Supplemental Figure I. The degree of fibrosis in HCM hearts (A) Representative cardiac magnetic resonance midventricular short-axis late gadolinium enhancement (LGE) image of an HCM patient showing hyperenhancement (yellow arrows) marking fibrotic areas in the left ventricular wall. Endocardial border (red line) and epicardial border (green line) of the LV are marked by manual contouring. The orange circle in the inferior wall provides a mean signal intensity for a representative region of normal myocardium. **(B)** The bar graph shows the percentage of myocardial delayed enhancement (MDE) fraction assessed by area of signal higher than 5 standard deviations of the signal from an area without delayed enhancement (orange circle in **A**). **(C)** Myocardium from HCM patients (n=7) and donors (n=7) stained with hematoxylin and eosin (H&E) for tissue morphology analysis; Masson's trichrome was used to mark collagenous fibrotic area in blue. Scale bar= 200μm. **(D)** Quantification of fibrosis using MIPAR software. Error bar represents mean ± SEM. Mann–Whitney U test was used in **D**. ***p<0.005. RV, right ventricle; LV, left ventricle.

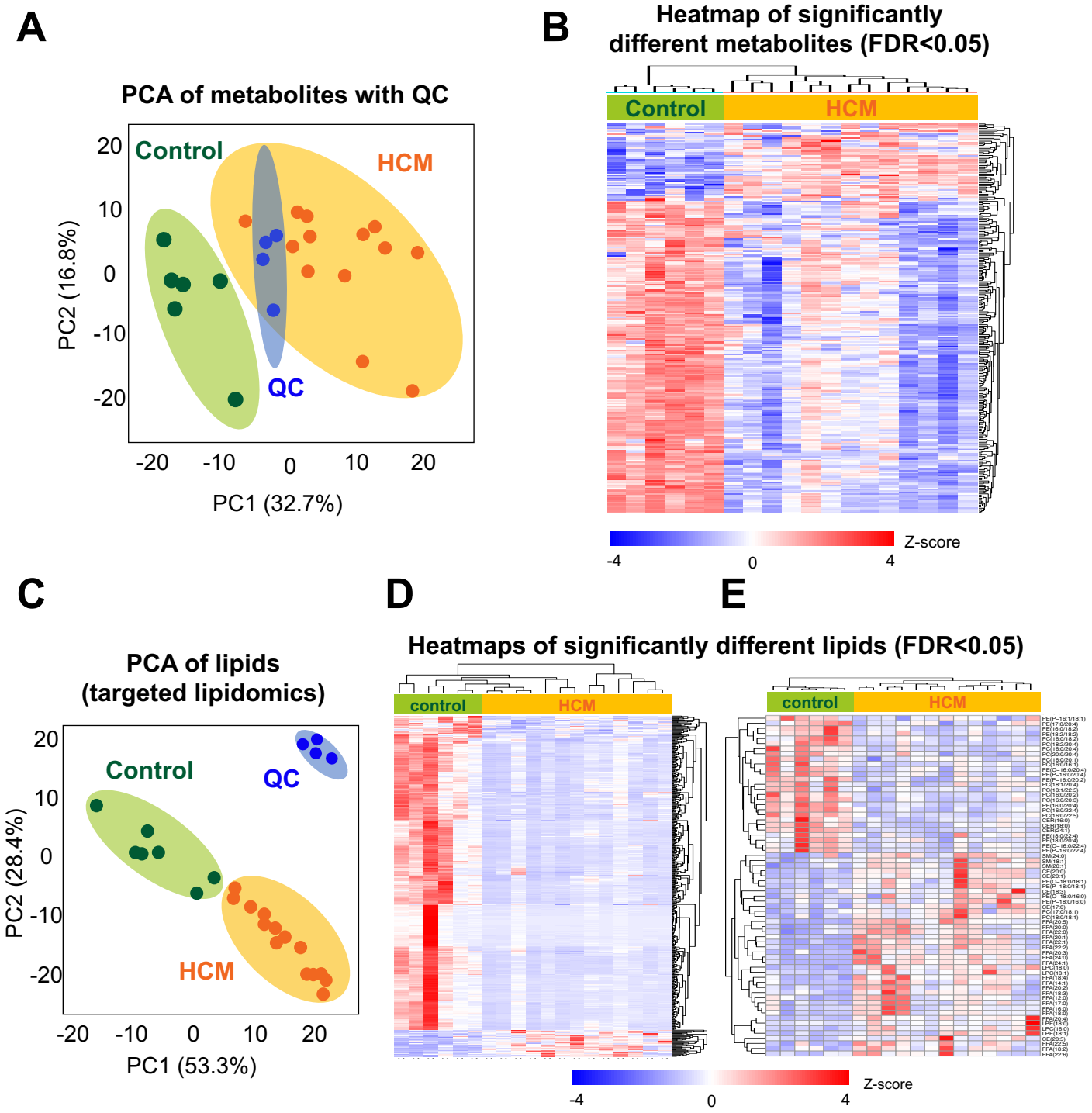

Supplemental Figure II. Distinct metabolome and lipid profile in HCM. (A) PCA plot shows global metabolic profile of all samples (HCM=13, control=6) and pooled samples for quality control (QC=5). **(B)** Clustering heatmap analysis of significantly changed metabolites (FDR<0.05) shows distinct metabolome in HCM. **(C)** Principal component analysis showing separation between HCM and control samples (donors and QCs) (HCM=13, control=6, QC=4). **(D)** Heatmap of significantly changed lipids (FDR<0.05) identified by targeted lipidomics. **(E)** Selected heatmap of significant lipids after excluding TAGs and DAGs. In all heatmaps, blue/red indicates a decrease/increase in metabolite level, respectively.

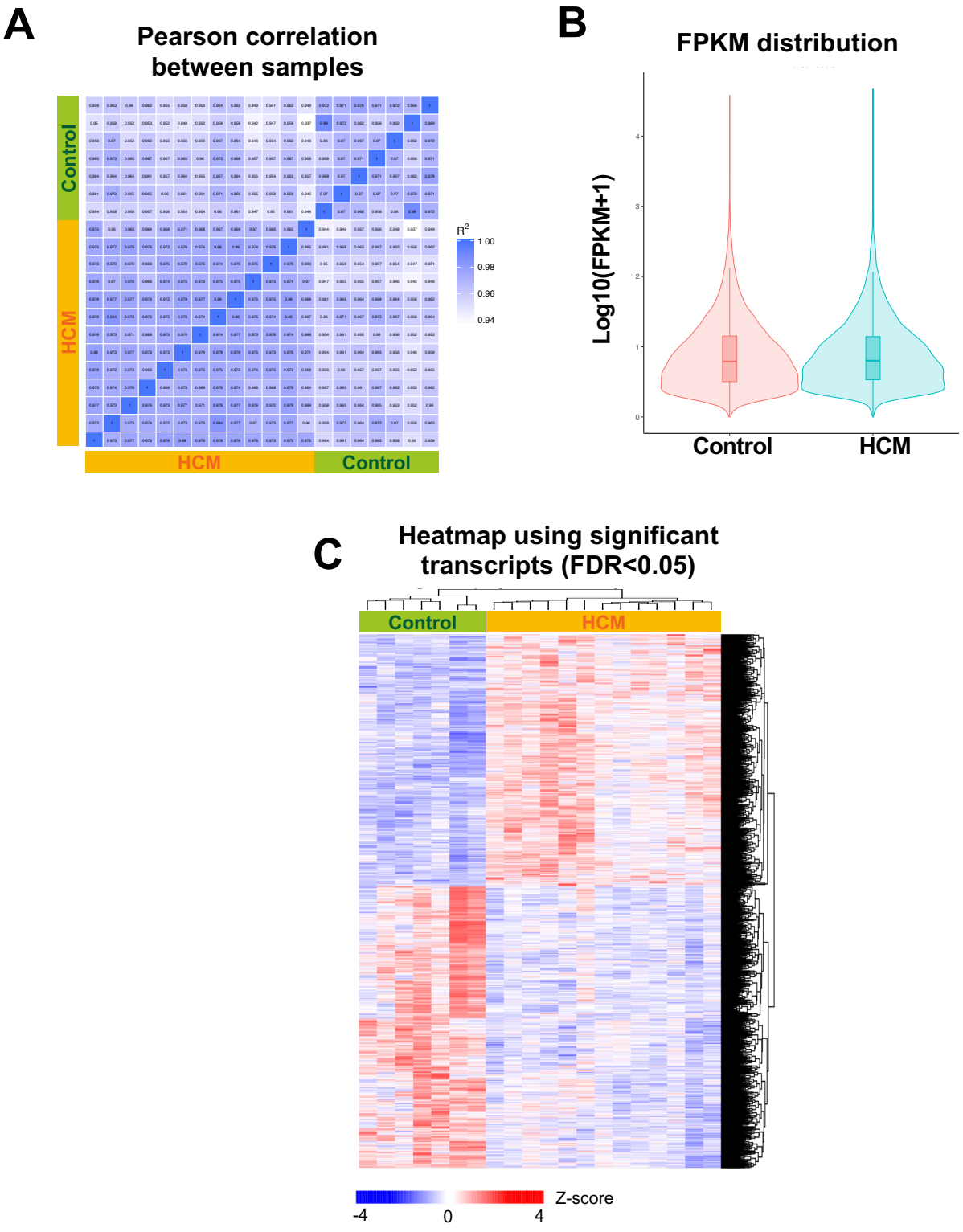

Supplemental Figure III. Differential transcriptomic profile in HCM. (A) The heatmap matrix shows the Pearson correlation coefficient between HCM and control (n=7 control and n=13 HCM). Darker blue represents relationships between samples that are most similar; white represents samples that are more dissimilar with lower coefficients. **(B)** Box plot shows distribution profile for all transcripts based on the fragments per kilobase of transcript per million mapped reads (FPKM). **(C)** Clustering heatmap analysis of significantly changed transcripts (FDR<0.05).

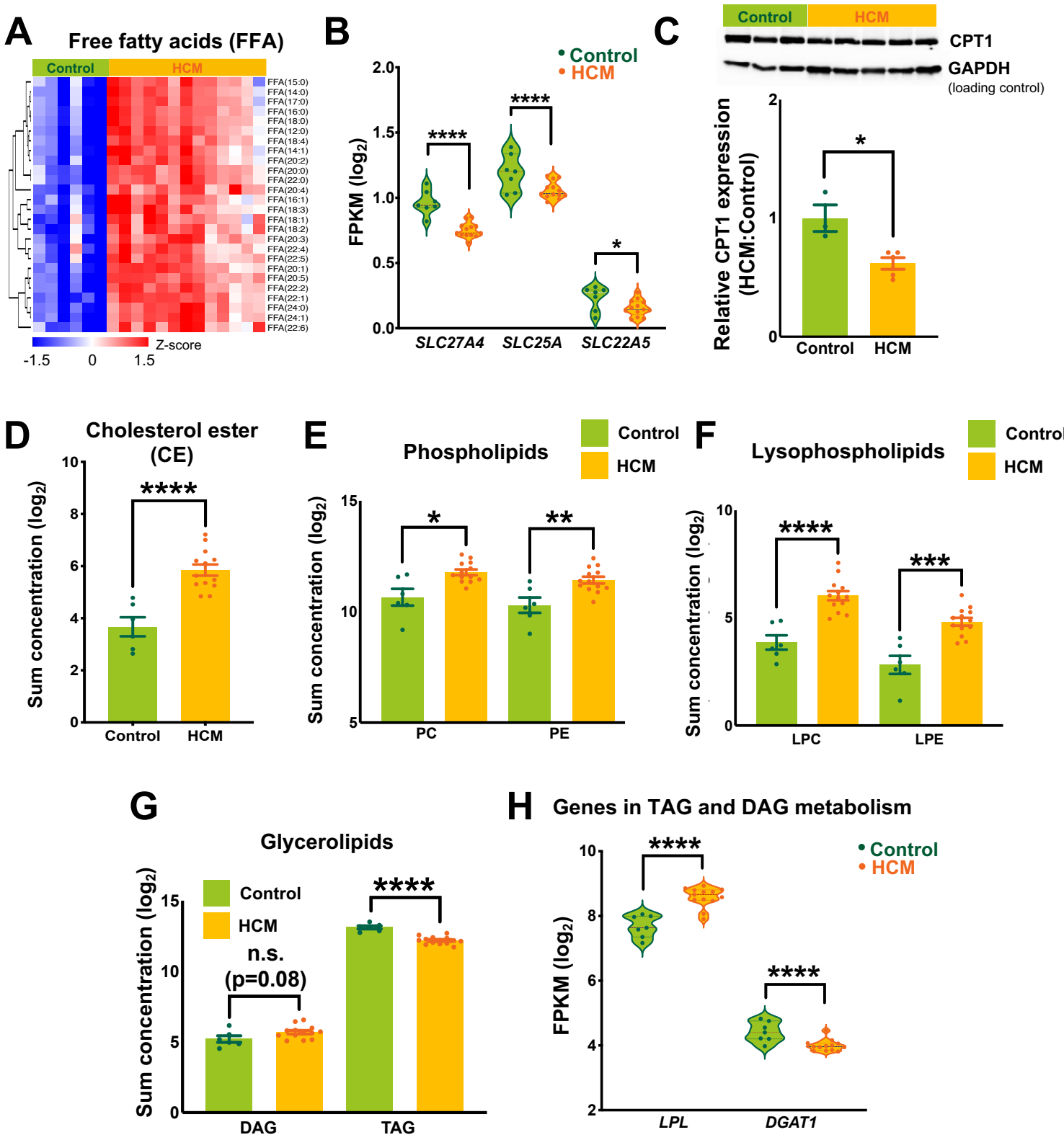
A
Free fatty acids (FFA)
Control
HCM
FFA(15:0)
FFA(14:0)
FFA(17:0)
FFA(16:0)
FFA(18:0)
FFA(12:0)
FFA(18:4)
FFA(14:1)
FFA(20:2)
FFA(20:0)
FFA(22:0)
FFA(20:4)
FFA(16:1)
FFA(18:3)
FFA(18:1)
FFA(18:2)
FFA(20:3)
FFA(22:4)
FFA(22:5)
FFA(20:1)
FFA(20:5)
FFA(22:2)
FFA(22:1)
FFA(24:0)
FFA(24:1)
FFA(22:6)
Z-score
-1.5
0
1.5
B
Control
HCM
FPKM (log2)
2.0
1.5
1.0
0.5
0.0
****
****
*
SLC27A4
SLC25A
SLC22A5
C
Control
HCM
CPT1
GAPDH
(loading control)
Relative CPT1 expression
(HCM:Control)
2
1
0
*
Control
HCM
D
Cholesterol ester
(CE)
Sum concentration (log2)
10
8
6
4
2
0
****
Control
HCM
E
Phospholipids
Control
HCM
Sum concentration (log2)
15
10
5
*
**
PC
PE
F
Lysophospholipids
Control
HCM
Sum concentration (log2)
10
5
0
****
***
LPC
LPE
G
Glycerolipids
Control
HCM
n.s.
(p=0.08)
Sum concentration (log2)
15
10
5
0
****
DAG
TAG
H
Genes in TAG and DAG metabolism
Control
HCM
FPKM (log2)
10
8
6
4
2
****
****
LPL
DGAT1

Supplemental Figure IV. Lipid dysregulation in HCM. (A) Heatmap shows free fatty acids (FFA) level measured by the targeted lipidomics platform. **(B)** Transcript level of lipid transporters (*SLC25A*, and *SLC22A5)* and CPT1 (*SLC27A4*) measured by RNA-Seq. **(C)** Representative western blot and quantification of CPT1 protein. GAPDH were used as a loading control**. (D-G)** Total concentration (log_2 scale) of CE, phospholipid, lysophopholipid, and glycerolipid measured by mass spec. **(H)** The transcript level of lipoprotein lipase (*LPL)* and diglyceride acyltransferase (*DGAT*) by RNA-Seq. Violin plot was reserved to show RNA-Seq data. Error bars represent mean ± SEM. n=6 control and n=13 HCM in **A** and **D-G**; n=7 control and n=13 HCM in **B** and **H**; n=3 control and n=5 HCM in **C**. Two-sided Welch's t-test or Wald test with Benjamini-Hochberg's FDR correction method used in **B** and **H**. Mann–Whitney U test was used in **C-G**. *p<0.05, **p<0.01, ***p<0.005, ****p<0.001 or n.s. not significant (p>0.05). FFA, free fatty acids; SLC, solute carrier family members; CE, cholesterol ester; PC, phosphatidylcholine; PE, phosphatidylethanolamine; LPC, lysophosphatidylcholine; LPE, lysophosphatidylethanolamine; DAG, diacylglycerol; and TAG, triacylglycerol.

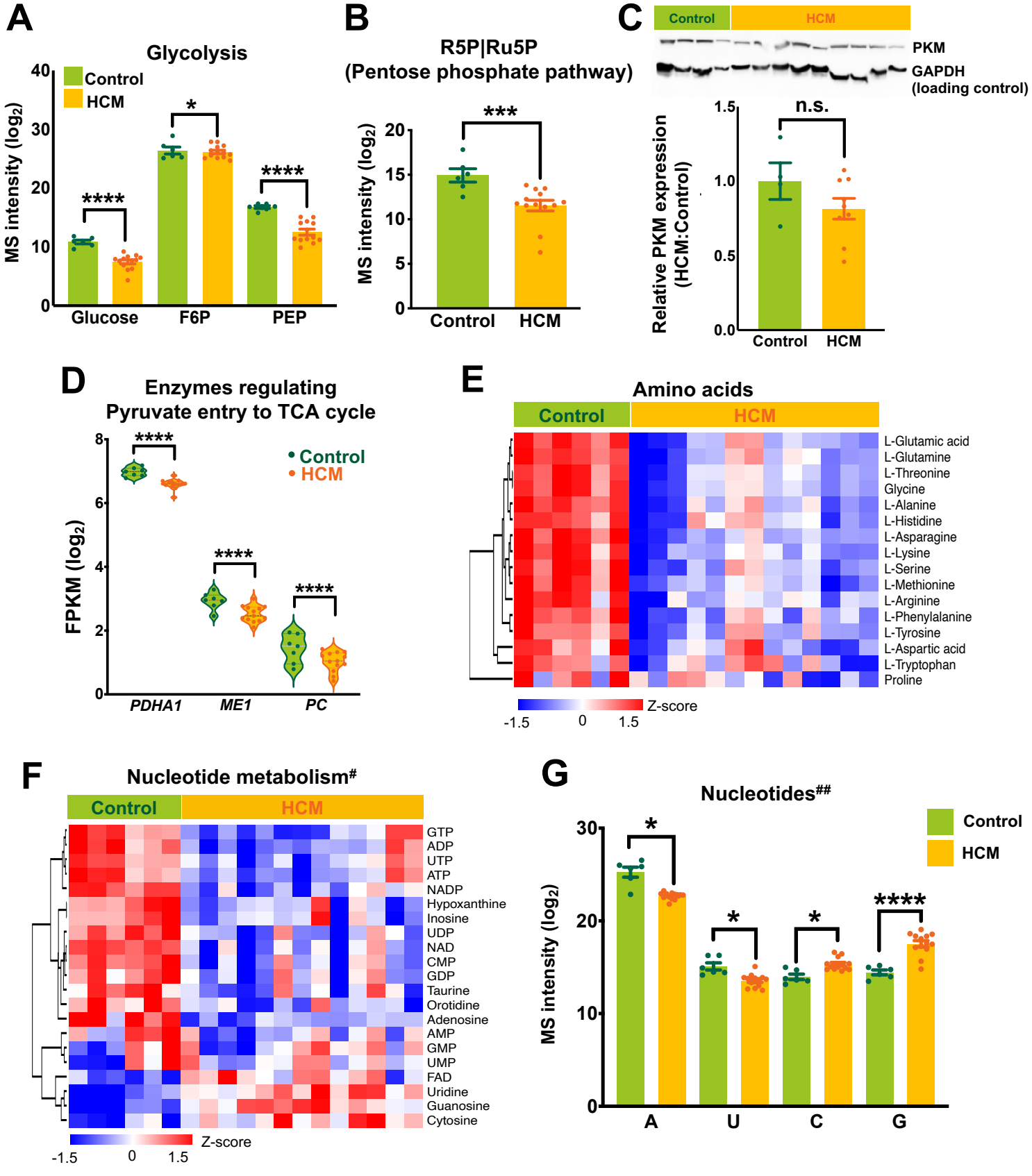
A
Glycolysis
Control
HCM
MS intensity (log2)
Glucose
F6P
PEP
B
R5P|Ru5P
(Pentose phosphate pathway)
MS intensity (log2)
Control
HCM
C
Control
HCM
PKM
GAPDH
(loading control)
Relative PKM expression
(HCM:Control)
n.s.
D
Enzymes regulating
Pyruvate entry to TCA cycle
FPKM (log2)
PDHA1
ME1
PC
E
Amino acids
L-Glutamic acid
L-Glutamine
L-Threonine
Glycine
L-Alanine
L-Histidine
L-Asparagine
L-Lysine
L-Serine
L-Methionine
L-Arginine
L-Phenylalanine
L-Tyrosine
L-Aspartic acid
L-Tryptophan
Proline
Z-score
F
Nucleotide metabolism#
GTP
ADP
UTP
ATP
NADP
Hypoxanthine
Inosine
UDP
NAD
CMP
GDP
Taurine
Orotidine
Adenosine
AMP
GMP
UMP
FAD
Uridine
Guanosine
Cytosine
Z-score
G
Nucleotides##
MS intensity (log2)
A
U
C
G

Supplemental Figure V. Dysregulated metabolites and their associated enzymes in HCM. (A and **B)** Glucose, intermediates of glycolysis, and pentose phosphate pathway metabolites measurements by mass spec. **(C)** Representative western blot and quantification of pyruvate kinase (PKM) showing a trend in deceased protein expression in HCM. GAPDH were used as a loading control**. (D)** Transcript level of enzymes regulating pyruvate entry to TCA cycle. **(E)** Heatmap shows significantly changed amino acids (FDR<0.05) in HCM. **(F** and **G)** Dysregulated metabolites (FDR<0.05) belonging to nucleotide metabolism. Violin plot was reserved to show RNA-Seq data. Error bars represent mean ± SEM. n=6 control and n=13 HCM in **A**, **B**, and **E-G**; n=4 control and n=9 HCM in **C**; n=7 control and n=13 HCM in **D**. Between-group comparisons performed using two-sided Welch's t-test or Wald test with Benjamini-Hochberg's FDR correction. *p<0.05, ***p<0.005, or ****p<0.001 or n.s. not significant (p>0.05). F6P, fructose 6-phosphate; PEP, phosphoenolpyruvic acid; R5P, Ribose 5 phosohate; Ru5P, Ribulose 5 phosphate; PDH, pyruvate dehydrogenase; ME, malic enzyme; PC, pyruvate carboxylase; A, adenine; U, uracil; C, cytosine; G, guanine. #CTP, cytosine triphosphate; CDP, cytosine diphosphate; TTP, thymidine triphosphate; and ##T, thymine were not detected.

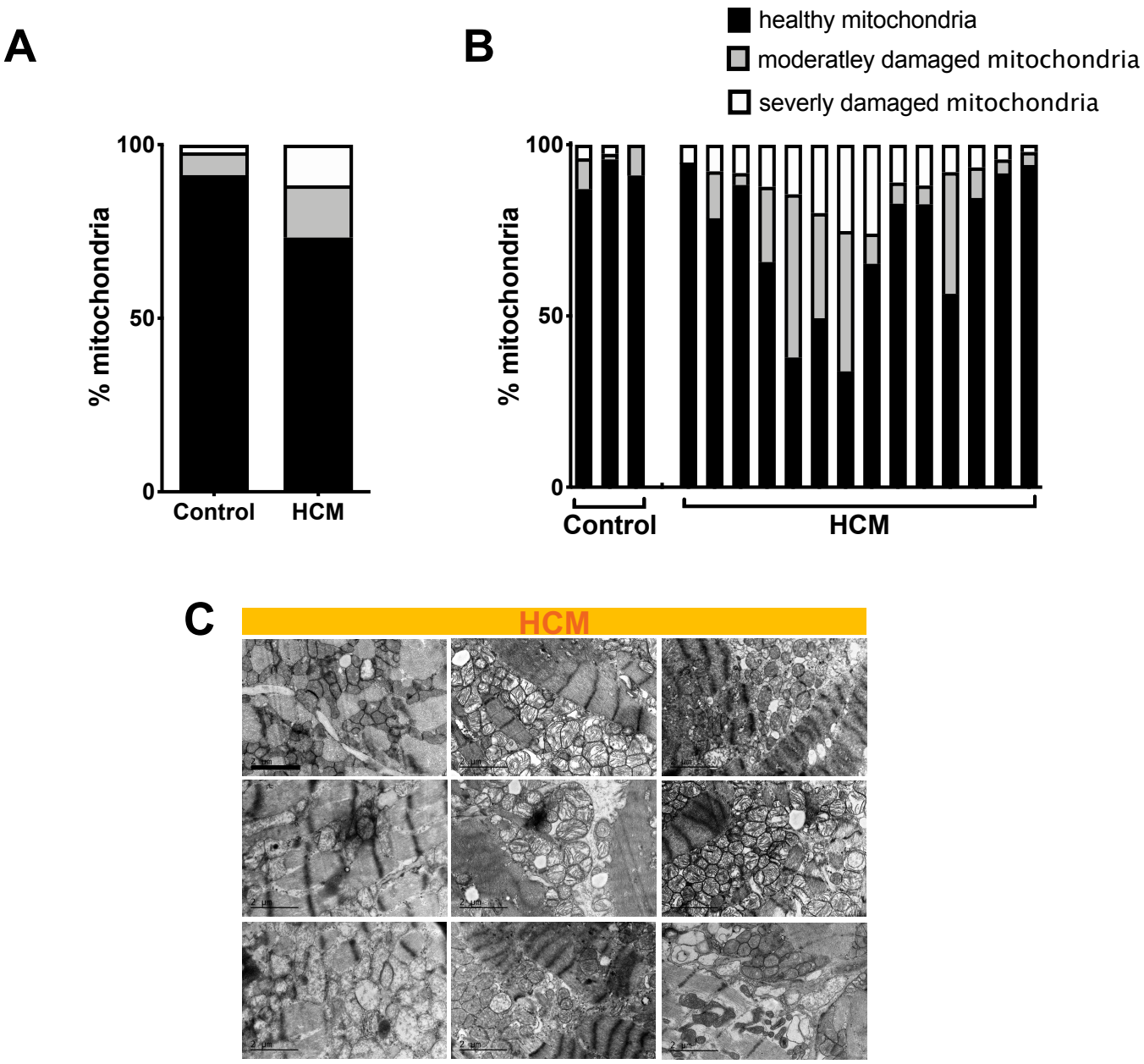

Supplemental Figure VI. Increased heterogeneity of mitochondrial cristae density in HCM. (A and **B)** Quantitative measurements of mitochondrial cristae density from EM micrographs using ImageJ presented as average of all data (A) or within each patient (B). About 20 randomly selected images from each sample were assessed. n=3 control and n=14 HCM. **(C)** Transmission electron microscope images of HCM patients showing mitochondrial heterogeneity within each sample (scale bar=2μm).

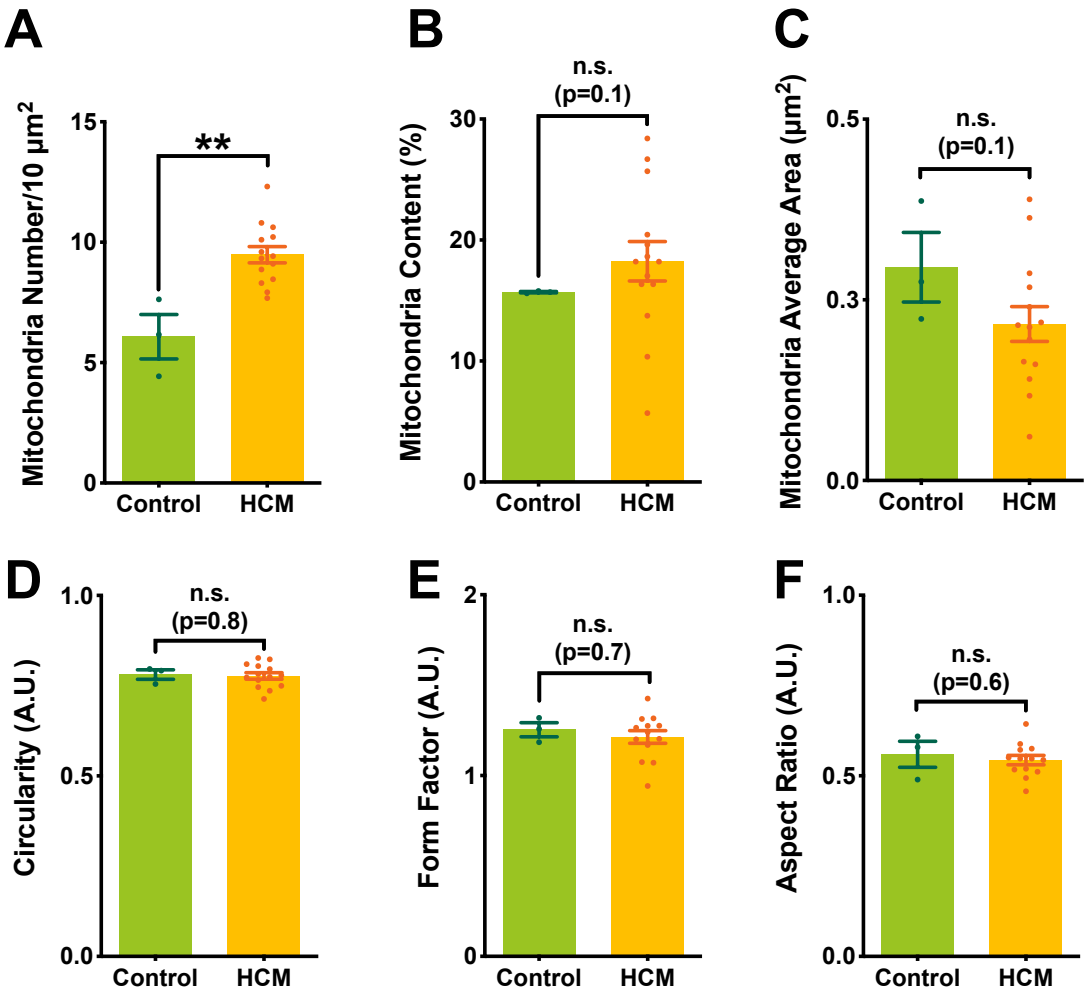

Supplemental Figure VII. Mitochondrial morphology in HCM. TEM micrographs were used to assess the following parameters in interfibrillar mitochondria of HCM and controls: **(A)** Total number of mitochondria per 10 µm^2, **(B)** mitochondrial content, **(C)** size, **(D)** circularity, **(E)** branching (form factor), and **(F)** ratio between major and minor mitochondrial axis (aspect ratio). A.U., arbitrary units. Error bars represent mean ± SEM. n=3 control and n=14 HCM. ~20 randomly selected images from each sample were assessed. Between-group comparisons performed using Mann–Whitney U test. **p<0.01 or n.s., not significant (p>0.05).

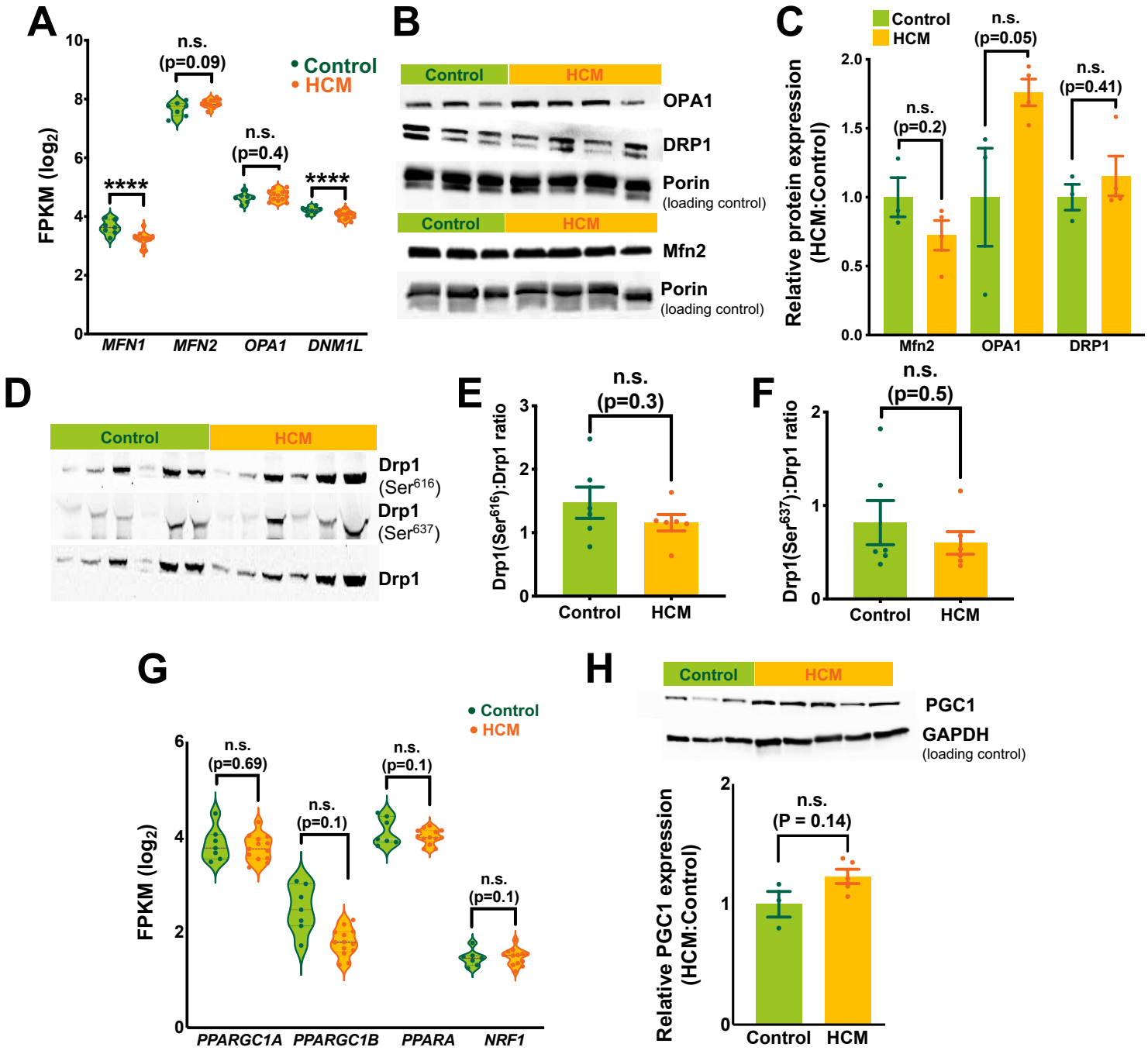

Supplemental Figure VIII. Mitochondrial dynamics and biogenesis. (A) Gene expression of mitochondrial dynamic regulators (*MFN1, MFN2, OPA1,* and *DNM1L*) by RNA-Seq. **(B** and **C)** Representative western blot and quantification of proteins regulating mitochondrial dynamics in mitochondrial fraction. Porin was used as a loading control. **(D-F)** Western blot and quantification of phosphorylated-Drp1 at Ser^{616} and Ser^{637} to total Drp1 ratio was assessed to examine activation or inhibition of mitochondrial fission, respectively. **(G)** Gene expression of mitochondrial biogenesis regulators by RNA-Seq. **(H)** Representative western blot and quantification of PGC1. GAPDH was used as a loading control. Violin plots were used to show RNA-Seq data. Error bars represent mean ± SEM. n=7 control and n=13 HCM in **A** and **G**; n=3 control and n=4 HCM in **B** and **C**; n=6 control and n=6 HCM in **D-F**; n=3 control and n=5 HCM in **H**. Between-group comparisons performed using Wald test and Benjamini-Hochberg's FDR correction method in **A** and **G**. Mann–Whitney U test used in **C**, **E**, **F** and **H**. ****p<0.001, or n.s, not significant. Ser, serine.

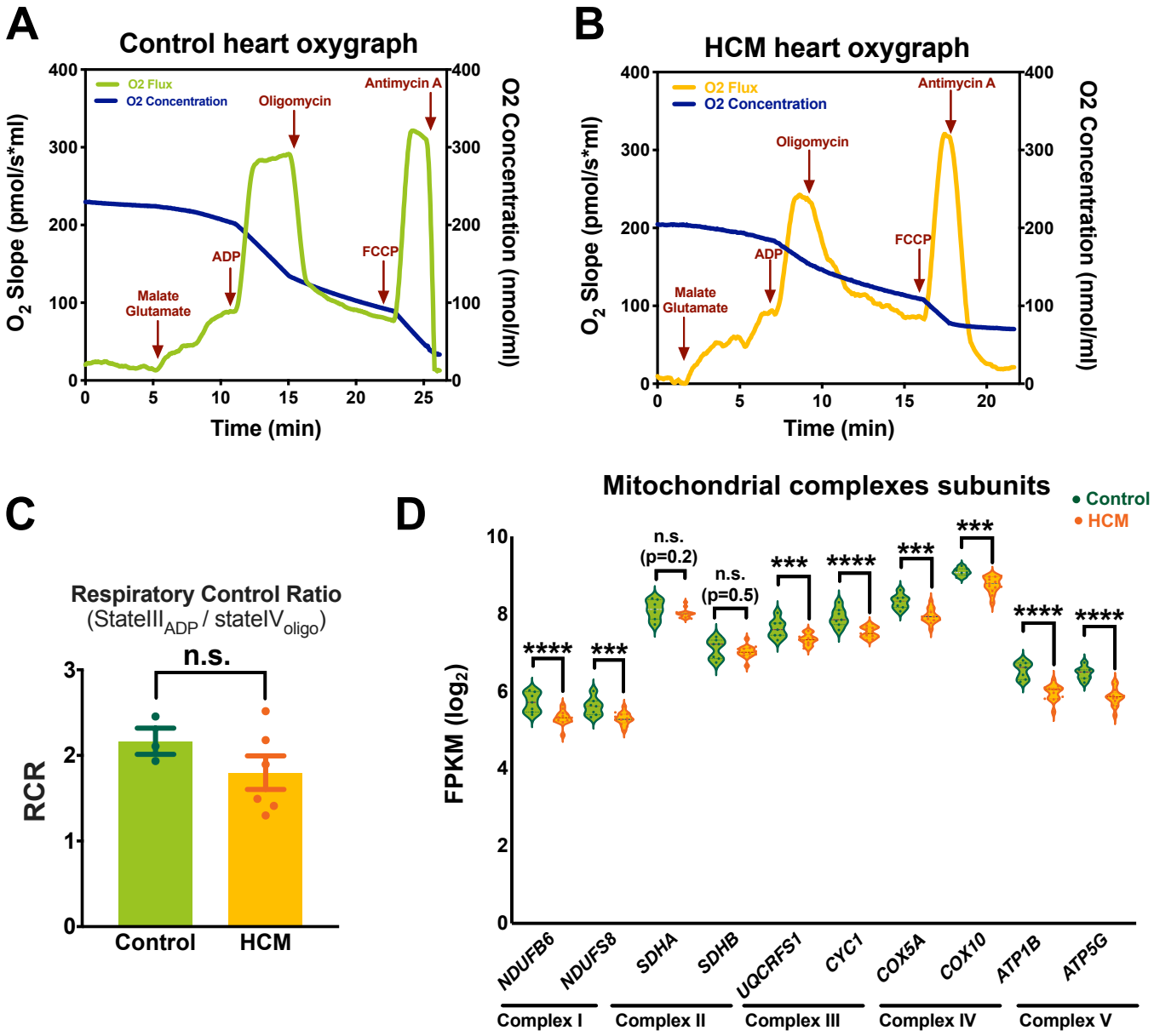

Supplemental Figure IX. Mitochondrial respiratory capacity in HCM. (A and **B)** Representative oxygraph traces showing respiratory activity in HCM and control. Arrows indicate the sequential additions of mitochondrial substrates to assess respiratory states in freshly isolated myocardial tissue. **(C)** Respiratory control ratio (RCR) was calculated as the ratio of state III (+ADP) to state IV (+Oligomycin). **(D)** Expression level of genes encoding multiple subunits of mitochondrial complexes in HCM and control. Violin plot was reserved to show RNA-Seq data. Error bars represent mean ± SEM. Between-group comparisons performed using Wald test and Benjamini-Hochberg's FDR correction method. n=3 control and n=9 HCM in **C**; n=13 control and n=7 HCM in **D**. ***p<0.005, or ****p<0.001, or n.s, not significant (p>0.05).

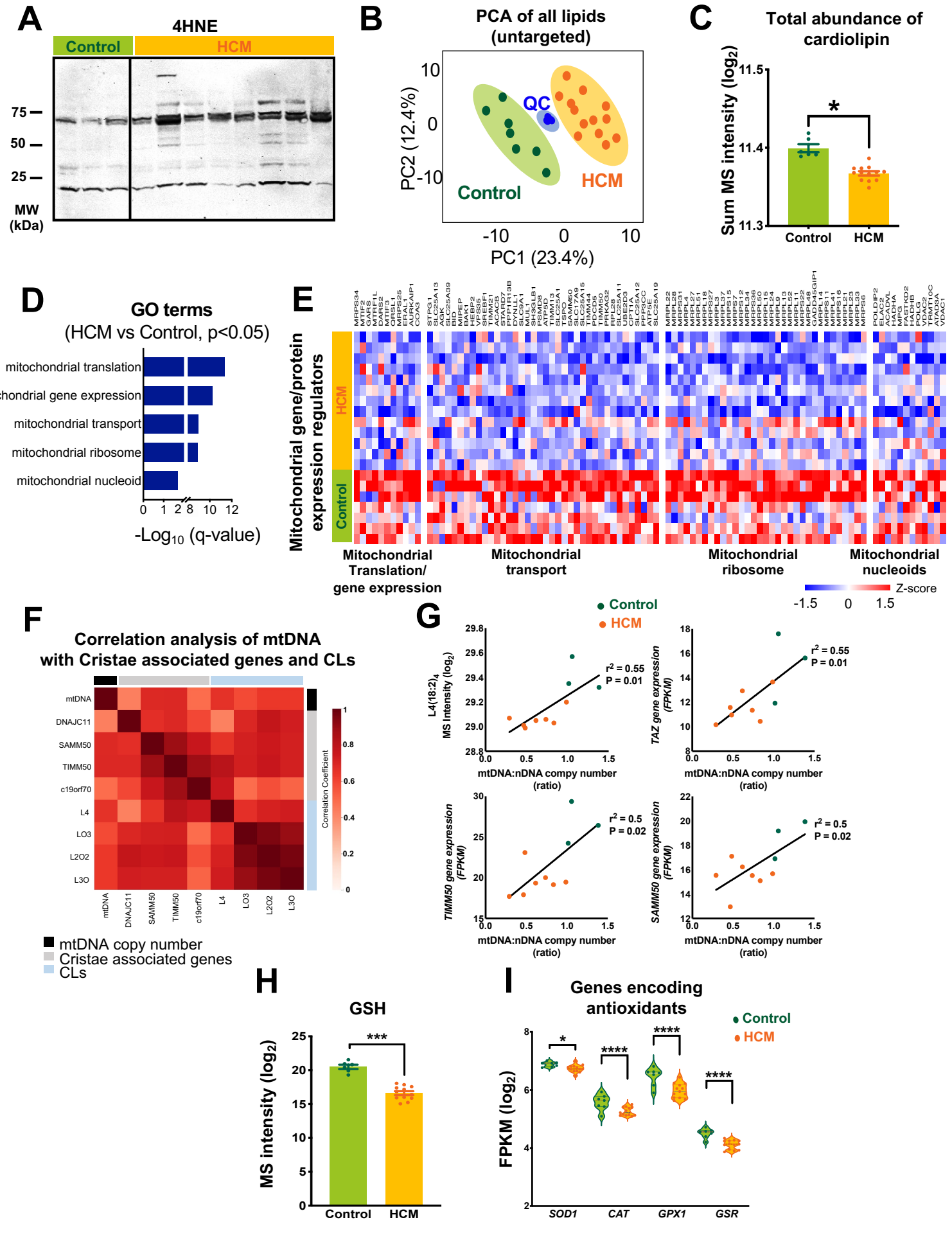
A
4HNE
Control
HCM
75
50
25
MW (kDa)
B
PCA of all lipids (untargeted)
QC
Control
HCM
PC2 (12.4%)
PC1 (23.4%)
C
Total abundance of cardiolipin
Sum MS intensity (log2)
Control
HCM
D
GO terms
(HCM vs Control, p<0.05)
mitochondrial translation
mitochondrial gene expression
mitochondrial transport
mitochondrial ribosome
mitochondrial nucleoid
-Log10 (q-value)
E
Mitochondrial gene/protein expression regulators
HCM
Control
Mitochondrial Translation/ gene expression
Mitochondrial transport
Mitochondrial ribosome
Mitochondrial nucleoids
Z-score
F
Correlation analysis of mtDNA with Cristae associated genes and CLs
mtDNA
DNAJC11
SAMM50
TIMM50
c19orf70
L4
LO3
L2O2
L3O
Correlation Coefficient
mtDNA copy number
Cristae associated genes
CLs
G
Control
HCM
L4(18:2)4 MS Intensity (log2)
r2 = 0.55
P = 0.01
mtDNA:nDNA compy number (ratio)
TAZ gene expression (FPKM)
r2 = 0.55
P = 0.01
TIMM50 gene expression (FPKM)
r2 = 0.5
P = 0.02
SAMM50 gene expression (FPKM)
r2 = 0.5
P = 0.02
H
GSH
MS intensity (log2)
***
Control
HCM
I
Genes encoding antioxidants
Control
HCM
FPKM (log2)
*
****
****
****
SOD1
CAT
GPX1
GSR

Supplemental Figure X. Oxidative damage in HCM. (A) Representative immunoblots of 4HNE. The signal intensity from ~65KD band was quantified in Figure 6A. Ponceau was used as a loading control. **(B)** PCA plot shows global lipid profile of all samples and plasma lipids as quality control (QC) samples identified by untargeted lipidomics. **(C)** Total concentration of cardiolipins measured by untargeted lipidomics. **(D)** Bar graph shows selected categories in GO enrichment analysis of mitochondrial genes measured by RNA-Seq **(E)** The expression of genes associated with mitochondrial gene expression, translation, transport, ribosomes, and nucleoids. **(F)** Heatmap of correlation matrix based on Pearson's coefficient between mtDNA copy number, genes associated with cristae formation/maintenance and different CL species. Correlation coefficients were shown with continuous gradient color (red), in which darker red represent higher correlation whereas lighter red indicate lower coefficients. mtDNA displayed in black, cristae genes are in light grey and CLs are marked in light blue. **(G)** Linear regression analysis of mtDNA copy number with Tetralinoleyl cardiolipin (L4) and the expression of genes associated with cristae formation/maintenance. **(H)** GSH level measured by mass spec. **(I)** The transcript level of key antioxidants measured by RNA-Seq. Violin plot was reserved to show RNA-Seq data. Error bars represent mean ± SEM. n=3 control, n=8 HCM in **A**; n=6 control, n=13 HCM in **B**, **C**, and **H**; n=7 control, n=13 HCM in **D**, **E** and **I**; control=3, HCM=7 in **F** and **G**. Between-group comparisons performed using Mann–Whitney U test in **C.** Two-sided Welch's t-test or Wald test with Benjamini-Hochberg's FDR correction method used in **H** and **I**. *p<0.05, ***p<0.005, or ****p<0.001.CL, cardiolipin; SOD, cytosolic superoxide dismutase; CAT, catalase; GPX, glutathione peroxidase; GSR, and glutathione reductase.

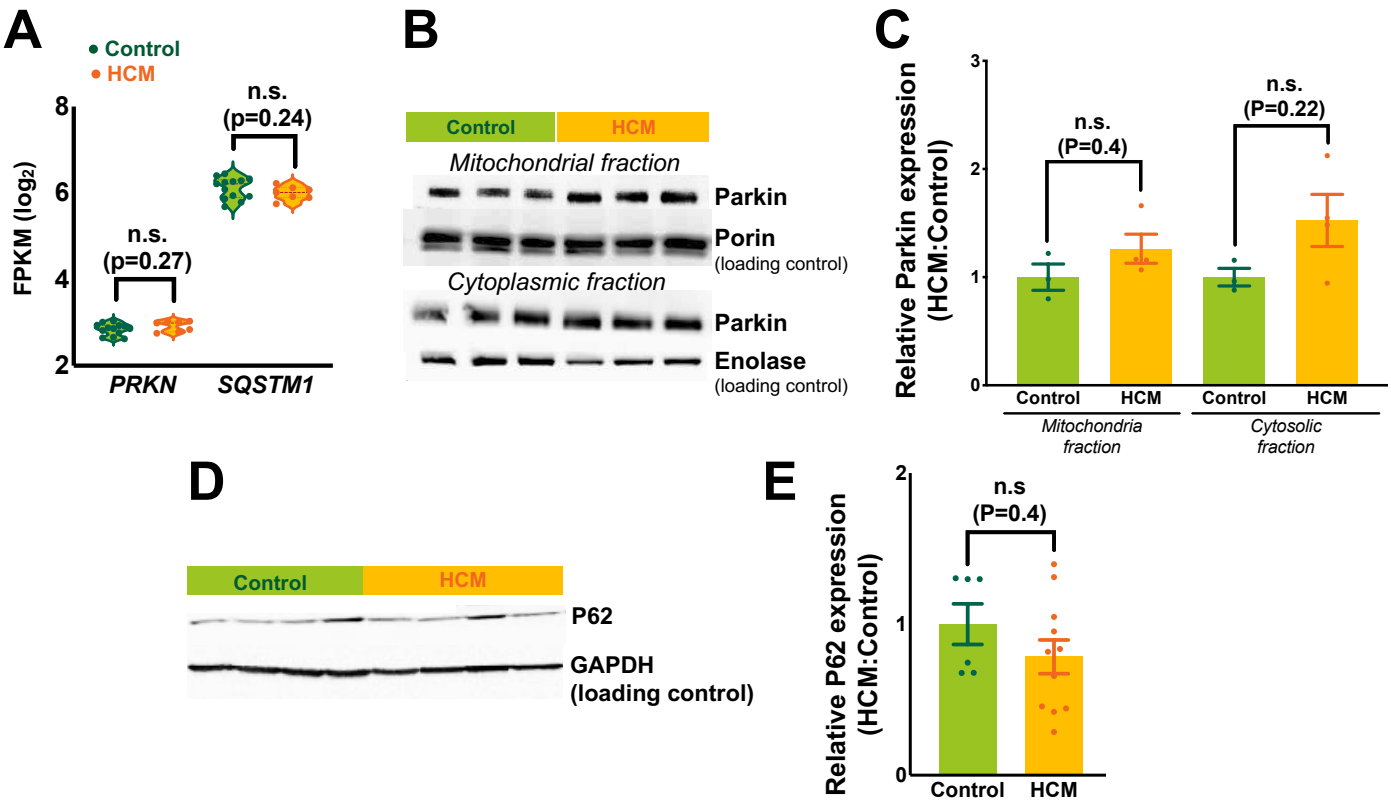

Supplemental Figure XI. Mitophagy in HCM. (A) The gene expression of Parkin (*PRKN*) and P62 (*SQSTM1*) measured by RNA-Seq. **(B** and **C)** Protein level and localization of Parkin, was measurand and quantified using Western blots analysis. Enolase and Porin were used as loading controls. **(D** and **E)** Representative blots and quantitative measurements of p62. GAPDH was used as a loading control. Violin plot was reserved to show RNA-Seq data. Error bars represent mean ± SEM. n=7 control and n=13 HCM in **A**. n=3 control and n=4 HCM in **B** and **C**; n=6 control and n=11 HCM in **D** and **E**. n.s, not significant (p>0.05).

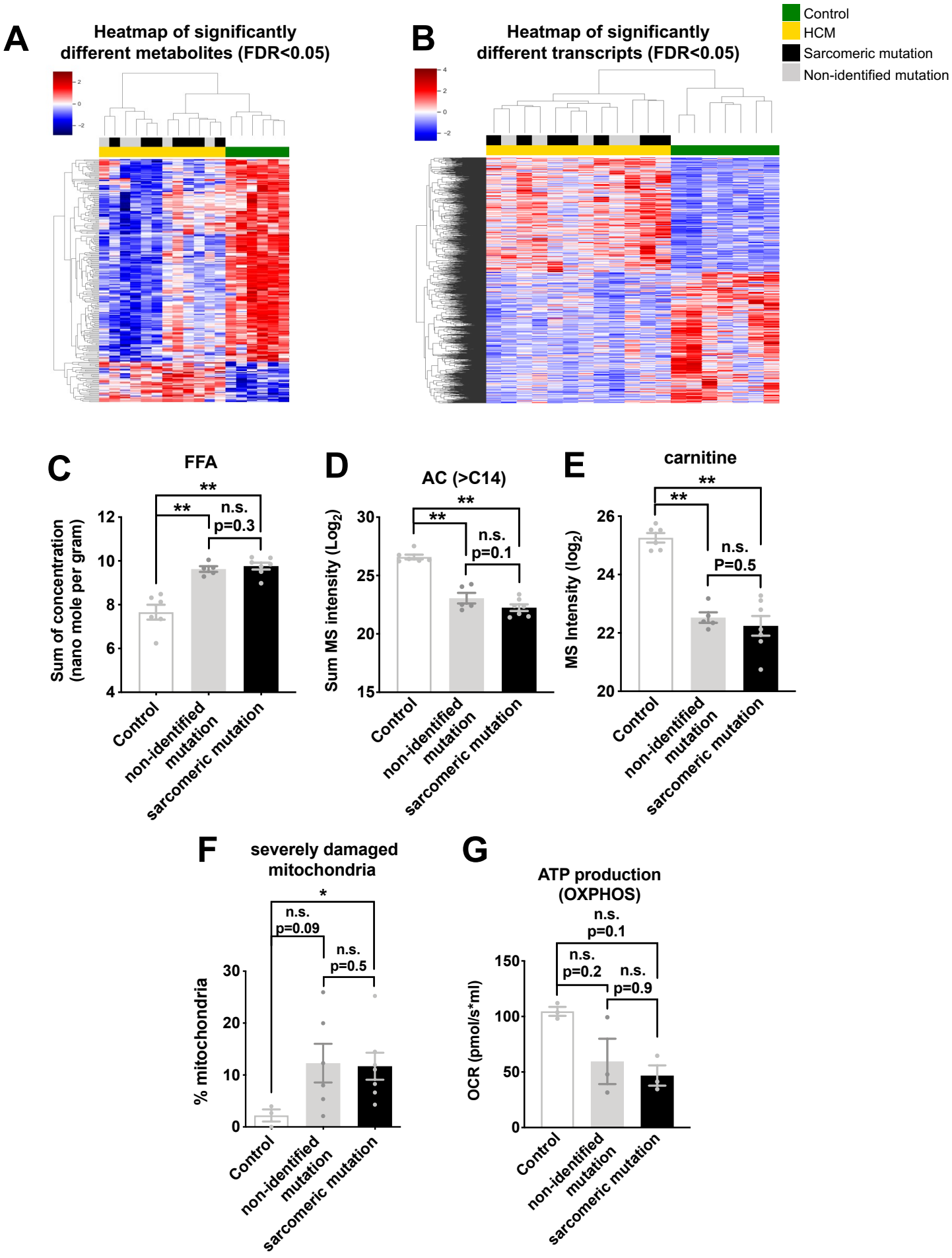
A
Heatmap of significantly different metabolites (FDR<0.05)
B
Heatmap of significantly different transcripts (FDR<0.05)
Control
HCM
Sarcomeric mutation
Non-identified mutation
C
FFA
Sum of concentration (nano mole per gram)
**
**
n.s.
p=0.3
D
AC (>C14)
Sum MS intensity (Log2)
**
**
n.s.
p=0.1
E
carnitine
MS Intensity (log2)
**
**
n.s.
P=0.5
Control
non-identified mutation
sarcomeric mutation
F
severely damaged mitochondria
% mitochondria
*
n.s.
p=0.09
n.s.
p=0.5
G
ATP production (OXPHOS)
OCR (pmol/s*ml)
n.s.
p=0.1
n.s.
p=0.2
n.s.
p=0.9

Supplemental Figure XII. The effect of sarcomeric mutations in HCM.
(A and **B)** Clustering heatmap analysis of significantly changed metabolites (FDR<0.05) and genes (FDR<0.05) in control, HCM patients with different sarcomeric causing mutations and non-identified mutation. As shown in the heatmap, HCM samples do not cluster based on the genotype. **(C-G)** Bar graphs show the analysis of mutations type and alteration in different molecular features: the level of FFA **(C)**, AC **(D)**, Carnitine **(E)**, % severely damaged mitochondria **(F)**, and ATP production **(G)**. n=6 control and n=7 HCM in (sarcomeric mutations) and n=5 (non-identified mutations) in **A**; n=7 control and n=7 HCM in (sarcomeric mutations) and n=5 (non-identified mutations) in **B**; n=6 control, n=7 (sarcomeric mutations) and n=5 (non-identified mutations) in **C-E**; n=3 control, n=7 HCM (sarcomeric mutations), and n=6 HCM (non-identified mutations) in **F**; n=3 in all groups in **G**. *p<0.05**,** **p<0.01 or n.s, not significant (p>0.05). One HCM patient with no available mutation information was excluded from the analysis.